



HAL
open science

Impurity transport and its modification by MHD in tokamak plasmas, with application to Tungsten in the WEST tokamak

P. Maget, J Frank, O. Agullo, X. Garbet, H. Lütjens

► **To cite this version:**

P. Maget, J Frank, O. Agullo, X. Garbet, H. Lütjens. Impurity transport and its modification by MHD in tokamak plasmas, with application to Tungsten in the WEST tokamak. 46th European Physical Society Conference on Plasma Physics (EPS 2019), Jul 2019, Milan, Italy. cea-02555120

HAL Id: cea-02555120

<https://cea.hal.science/cea-02555120v1>

Submitted on 27 Apr 2020

HAL is a multi-disciplinary open access archive for the deposit and dissemination of scientific research documents, whether they are published or not. The documents may come from teaching and research institutions in France or abroad, or from public or private research centers.

L'archive ouverte pluridisciplinaire **HAL**, est destinée au dépôt et à la diffusion de documents scientifiques de niveau recherche, publiés ou non, émanant des établissements d'enseignement et de recherche français ou étrangers, des laboratoires publics ou privés.

Impurity transport and its modification by MHD in tokamak plasmas, with application to Tungsten in the WEST tokamak

P. Maget, J. Frank¹, O. Agullo¹, X. Garbet, H. Lütjens², and the WEST team³

CEA, IRFM, F-13108 Saint Paul-lez-Durance, France.

¹ *Aix-Marseille Université, CNRS, PIIM UMR 7345, 13397 Marseille Cedex 20, France.*

² *Centre de Physique Théorique, Ecole Polytechnique, CNRS, France.*

³ *see <http://west.cea.fr/WESTteam>*

Summary The neoclassical transport of impurities is investigated analytically and numerically in this work, and the effect of a magnetic island for a WEST plasma is described. It is shown that the poloidal asymmetry of the impurity density can be described with a simple analytical model, and numerical simulations with a non linear fluid code confirm the analytical findings. The poloidal asymmetry tends naturally to cancel as the impurity profile evolves towards its steady state. When a magnetic island is present, temperature screening is lost locally above a critical island size. Tungsten transport is however dominated by turbulence on WEST. Simulations with a turbulent transport model confirm that the Tungsten profile is flat, as observed, but that the poloidal asymmetry remains close to its neoclassical value.

The transport of impurities in tokamak plasmas is a key issue in fusion research, since both plasma facing components and fusion reactions introduce undesirable ions in the fusion mixture that radiate plasma energy and dilute the fusion reactants. This transport can be separated into a collisional (neoclassical) and a turbulent component. The neoclassical impurity transport is extremely sensitive to the poloidal anisotropy of the impurity density [1]. We show that this poloidal asymmetry can be determined analytically from equilibrium profiles and that impurity fluxes are strongly modified even in the absence of toroidal rotation. The asymmetry is parametrized by a horizontal (δ) and vertical (Δ) components: $n_a / \langle n_a \rangle = 1 + \delta \cos \theta + \Delta \sin \theta$ with n_a the impurity density and θ the poloidal angle.

Neoclassical transport with self-consistent poloidal asymmetry The neoclassical radial impurity flux writes

$$\langle \Gamma_a \cdot \nabla r \rangle \approx - \langle n_a \rangle D_{PS}^a \left[\left(1 + \frac{\delta}{\varepsilon} + \frac{\delta^2 + \Delta^2}{4\varepsilon^2} \right) G + \frac{1}{2} \left(\frac{\delta}{\varepsilon} + \frac{\delta^2 + \Delta^2}{2\varepsilon^2} \right) U \right] \quad (1)$$

with $D_{PS}^a \equiv 2q^2 m_a \nu_a T_a / (e_a^2 \langle B^2 \rangle)$ and

$$G = \partial_r \ln p_a - \frac{e_a T_i}{e_i T_a} \partial_r \ln p_i + C_0^a \frac{e_a T_i}{e_i T_a} \partial_r \ln T_i, \quad U \approx - (C_0^a + k_i) \frac{e_a T_i}{e_i T_a} \partial_r \ln T_i \quad (2)$$

The poloidal asymmetry parameters (δ, Δ) verify

$$\Delta^2 + (\delta - C_\delta)^2 = R_\Delta^2 \quad (3)$$

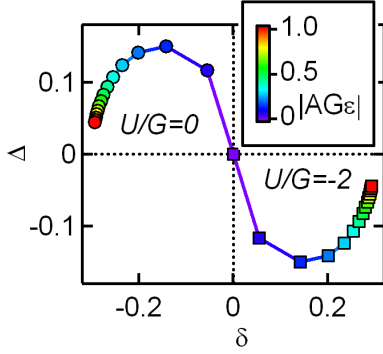


Figure 1: *Poloidal asymmetry in the (δ, Δ) plane for a peak (left) and flat (right) ion density cases.*

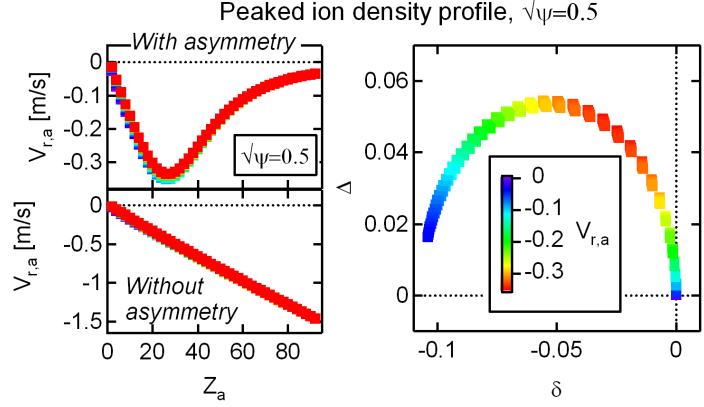


Figure 2: *Radial velocity as a function of the ion charge (left plot), with (top) and without (bottom) poloidal asymmetry, and radial velocity (in [m/s]) in the (δ, Δ) plane (right plot), for a peaked ion density profile, and a flat impurity profile.*

which describes a circle of center C_δ and radius R_Δ with $C_\delta = -\varepsilon / (1 + U/G)$ and $R_\Delta = |C_\delta|$. Defining $\delta = C_\delta + R_\Delta \cos \alpha$ and $\Delta = R_\Delta \sin \alpha$, the angle α on the circle can be determined:

$$\cos \alpha = \frac{R_\Delta (AG\varepsilon)^2 - R_\Delta^2}{C_\delta (AG\varepsilon)^2 + R_\Delta^2}, \quad \sin \alpha = 2R_\Delta \frac{AG\varepsilon}{(AG\varepsilon)^2 + R_\Delta^2} \quad (4)$$

with $A = (Rq/r)^2 Rv_a / \omega_{c,a} \propto Z_a$: the angle α is an increasing function of the collision frequency between the impurity and the main ion. When the ion density profile is peaked, $C_\delta < 0$ and Δ is positive, while a flat ion density profile will give $C_\delta > 0$ and $\Delta < 0$ (fig. 1). For a flat impurity profile, the maximum radial transport will concern medium- Z impurities in the range 20-30, for which the vertical asymmetry is also the largest (fig. 2).

Numerical simulations of neoclassical impurity transport Numerical experiments are performed with the non linear MHD code XTOR-2F [2] where neoclassical physics is implemented [3]. The model is completed with two additional equations per impurity:

$$\partial_t n_a + \nabla \cdot (n_a \mathbf{V}_a) = -\nabla \cdot \Gamma_a^{turb} \quad (5)$$

$$m_a n_a D_t V_{a\parallel} = -\nabla_{\parallel} p_a + n_a e_a E_{\parallel} + R_{a\parallel} - (\nabla \cdot \Pi_a)_{\parallel} \quad (6)$$

with $D_t \equiv \partial_t + [(V_{\parallel a} \mathbf{b} + \mathbf{V}_E) \cdot \nabla V_{\parallel a} \mathbf{b}] \cdot \mathbf{b}$, $\mathbf{V}_a = \mathbf{V}_{\parallel a} + \mathbf{V}_a^*$ and $\Gamma_a^{turb} = -D_a \nabla n_a$. We assume $E_{\parallel} \approx -\nabla_{\parallel} p_e / (en_e)$, $R_{a\parallel}$ is the parallel component of the collisional friction force and $(\nabla \cdot \Pi_a)_{\parallel}$ is the parallel component to the anisotropic pressure tensor. We consider a circular cross section equilibrium with a peak or a flat ion density profile, and a profile of Tungsten W^{44+} that is initially flat. The collision frequency ν_a can be artificially amplified in order to test the analytical model, and the anomalous diffusion coefficient (D_a) is kept very low. We show in fig. 3 and 4

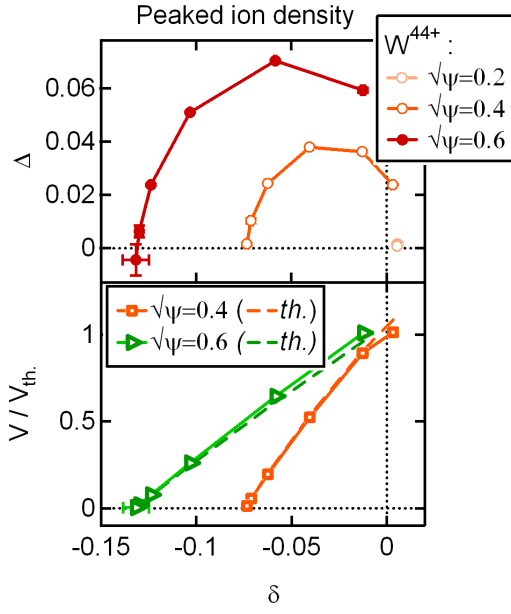


Figure 3: *Collisionality scan for the peak ion density case: trajectory of the poloidal asymmetry (top), and radial velocity normalized to its value without asymmetry (bottom).*

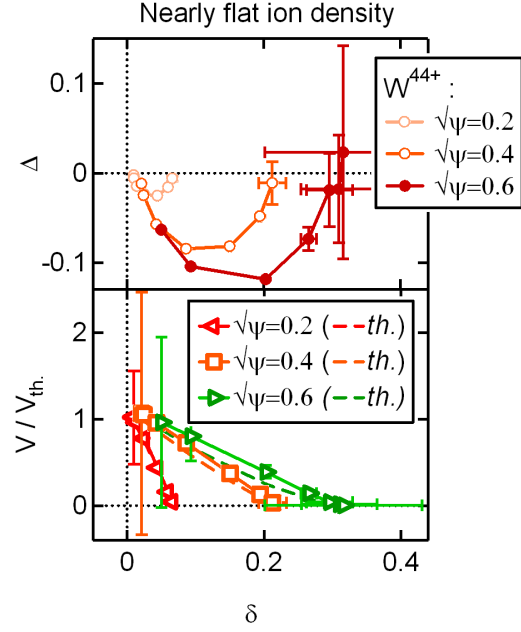


Figure 4: *Collisionality scan for the flat ion density case: trajectory of the poloidal asymmetry (top), and radial velocity normalized to its value without asymmetry (bottom).*

the result of this collisionality scan for the two different ion density profiles. The asymmetry describes the expected circles, and the radial flux follows the prediction from theory. It is damped in the two cases by the natural poloidal asymmetry.

Neoclassical impurity transport in presence of a (2,1) island on WEST Magnetic islands are observed to modify impurity transport in experiments, and the loss of temperature screening is suspected to be instrumental in this correlation [4]. We consider a typical WEST plasma from the 2018 experimental campaign, with a resonant surface $q = 2$ relatively close to the plasma edge, at $\sqrt{\bar{\psi}} = 0.8$. The natural saturated size of the (2,1) island is $W = w/a \approx 4\%$, but a scan in the island size can be performed by inserting a larger seed and by following the evolution of the Tungsten transport at different stages of the island decay. The dependence of the radial flow of Tungsten on the (2,1) island width is shown in fig. 5. Without island, the radial flux is nearly zero ($V_{r,W}^0$), and it increases towards its predicted value without temperature screening ($V_{r,W}^{isl}$) as the island size becomes larger than the characteristic transport width W_χ [5]. A fit using the tanh function gives a satisfactory transition between the local Tungsten velocity with and without a magnetic island, with a transition starting at $W \sim W_\chi$:

$$V_{r,W} = V_{r,W}^0 + V_{r,W}^{isl} \times \left[1 + \tanh 3 (W - 1.8W_\chi) / W_\chi \right] \quad (7)$$

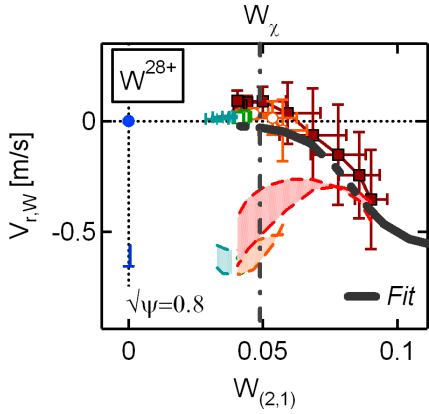


Figure 5: Radial Tungsten velocity at the island position as a function of its size. Colored area: without temperature screening.

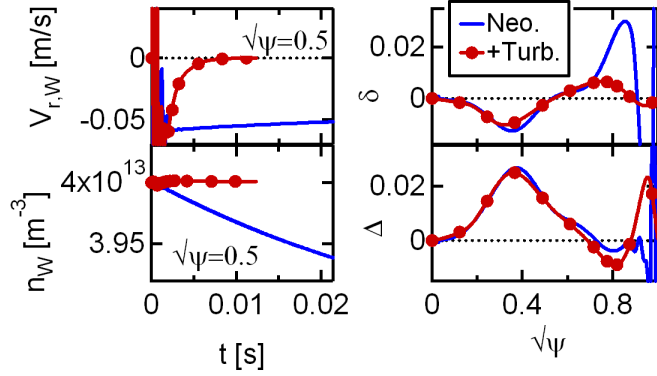


Figure 6: Effect of turbulence on Tungsten transport: radial velocity and density evolution at $\sqrt{\psi} = 0.5$ (left); profiles of (δ, Δ) (right).

Turbulent impurity transport on WEST In WEST, it has been found using the Qualikiz code [6] that Tungsten transport is in fact dominantly turbulence-driven [7]. The anomalous impurity transport model has therefore been complemented with a turbulent pinch that includes thermo-diffusion and curvature terms:

$$\Gamma_a^{turb} = -D_{\perp}^a \nabla n_a + n_a \mathbf{V}_p^a, \quad \mathbf{V}_p^a = D_{thd}^a \nabla \ln T_a + \mathbf{V}_{cur}^a \quad (8)$$

where we take from Qualikiz results $D_a = 8m^2/s$, $D_{thd}^a = 0.8m^2/s$ and $V_{cur}^a = -6.7m/s$, much above neoclassical values. As shown in fig. 6, the Tungsten flux rapidly equilibrates with a flat radial profile, as suggested by experimental observations. But the poloidal asymmetry does not seem to respond strongly, and remains comparable to its neoclassical value. Simulations with a magnetic island have not been performed yet in presence of turbulence. This will imply using a transport model where turbulence cancels inside the island [8].

References

- [1] C. Angioni and P. Helander, Plasma Physics and Controlled Fusion **56** (2014) 124001.
- [2] H. Lütjens and J.F. Luciani, Journal of Computational Physics **229** (2010) 8130 .
- [3] P. Maget et al., Nuclear Fusion **56** (2016) 086004. ; Nuclear Fusion **59** (2019) 049501.
- [4] T. Hender et al., Nuclear Fusion **56** (2016) 066002.
- [5] R. Fitzpatrick, Physics of Plasmas **2** (1995) 825.
- [6] C. Bourdelle et al., Physics of Plasmas **14** (2007) 112501
- [7] C. Bourdelle et al., this conference **O5.101** X. Yang et al., this conference **P5.1085**
- [8] P. Maget et al., Plasma Phys. and Cont. Fus. **60** (2018) 095003.